

COMBINED APPROACHES TO LIGHTWEIGHT ARM UTILIZATION

W. J. Book, S. L. Dickerson, G. Hastings, S. Cetinkunt, and T. Alberts
School of Mechanical Engineering
Georgia Institute of Technology
Atlanta, Georgia

ABSTRACT

In order to use lightweight arms the combination of a number of new approaches in arm design and control may be necessary. This paper describes four complimentary research efforts and how their results will work together. The bracing strategy is proposed first as one scenario of arm usage. It braces the arm against a passive structure to increase rigidity during fine motions of the end effector. Large motions of the arm require path and trajectory planning. Research on minimum time motions that avoid unnecessarily exciting vibrations is described next. The damping of those vibrations that are excited can be accomplished through a combination of active modal feedback control and passive damping. The enhancement of the damping characteristics of arm structures is described. This is important for stable feedback control with actuators and controllers with limited bandwidth. Analytical and experimental results for constrained layer damping are described in the context of the control problem. An active modal control has been implemented on a simple one link beam. As higher bandwidth is sought from this physical system deviations from the predicted results were observed. A refinement of the model to include anti-aliasing filter, sample-data, and amplifier effects explains the behavior as explained.

INTRODUCTION

The performance of manipulator arms must be defined in the context of the task the arm. Speed, accuracy, dexterity, weight, complexity, and reliability are some of the dimensions of the performance measure. One fundamental issue in the design of arms is the arm rigidity and the interaction of the control system with the dynamics of the arm its actuators and sensors. The limitations on controlling a flexible motion system certainly limit the performance of robot arms designed today. Research to understand and overcome these limitations is an important component of extending overall robot performance in several of the dimensions mentioned above.

This material is based in part on work supported by the National Science Foundation under grant MEA-8303539 and by the Georgia Tech Material Handling Research Center.

In an effort to make lighter robot arms feasible, and hence determine their desirability, several complimentary approaches can be taken together. This paper describes research underway investigating these approaches separately and in combination. The separate approaches are:

1. Feedback control of flexible state variables.
2. Enhanced passive damping of flexible modes.
3. Path and trajectory planning to constrain excitement of the flexible modes.
4. The bracing strategy to rigidize the base of the "wrist" for subsequent fine motions.

Notably absent from consideration are studies of more rigid arm configurations and materials. It appears that the consequences of these approaches to designing lighter arms are better understood and somewhat decoupled from the issues under study here. They could be incorporated with the approaches under study in a commercial design.

The present paper will briefly describe all four approaches listed and the interactive roll they play. The references listed will provide more detail on the individual approaches.

THE BRACING STRATEGY

The small, high bandwidth motions often required for precision manipulation tasks are called fine motions. The high bandwidth and accuracy needed for fine motions are principal reasons arm rigidity has been sought in existing designs. While more complex controls can theoretically provide this behavior even in lightweight arms, practical problems of disturbance rejection and plant uncertainty encourage us to seek alternatives. The bracing strategy [1] achieves large configuration changes (gross motion) with the lightweight arm, followed by bracing the arm near its end against a passive bracing structure. This structure may be provided explicitly for that purpose or it may consist of the work piece itself. The rigidity of the lightweight arm is now supplemented with the rigidity of the bracing structure. Subsequent fine motions take place at additional degrees of freedom past the bracing point. They have the benefit of a fairly rigid base and typically a shorter chain of links. The control of the fine motions might ignore the effects of flexibility for this reason.

The fine motions of the braced end effector are not the subject of this paper. Suffice it to say that the bracing action may compromise the accuracy of the end effector location relative to the arm base. Control of the fine motion based on sensing the end effector's position and perhaps force relative to the work piece becomes even more important with the bracing strategy.

In order to apply the bracing strategy one must obtain certain capabilities. First, the light weight arm must be moved rapidly over a large configuration change. Secondly, the arm must be brought into a controlled collision with the bracing structure which positions the end effector accurately enough and does not damage the arm or work piece. Finally, a bracing action must occur. This action may be the application of force normal to the bracing surface to achieve adequate friction to avoid slipping. Alternatively, it could be actuation of a suction or magnetic attachment.

Integration Of Design And Control Approaches

Using the bracing strategy as the scenario of arm operation, the role of the remaining three approaches first listed will now be established.

During a rapid configuration change the precise position of the arm is not usually of concern until the end of the path. As the end of the path is approached it is important to avoid collisions and to facilitate the second phase: the docking with the bracing structure. Both needs are served if the configuration change is completed with minimal excitation of the flexible degrees of freedom, though this must be completed in minimum time. The path of the arm in the work space must avoid obstacles which may dictate the general nature of the path. If we assume the arm deflection is small relative to the clearance allowed in the path, the joint histories alone are sufficient to guarantee no collisions. Our minimum time control research first assumes that the joint angles are prescribed as a function of an independent path variable, s . One is only allowed to alter the velocity along the path, ds/dt , to improve the arm performance. The second phase is to modify the joint histories to improve the performance at critical points in the motion.

At the end of a configuration change additional small arm motions are needed to accomplish bracing. It may be preferable not to use bracing in some applications, in which case these motions constitute the fine motions of the task. The system is not changing configuration so a linear controller is a good candidate for this application. It must have a relatively high bandwidth and must act to damp out the flexible modes. A linear optimal regulator has been studied analytically and experimentally for this purpose. Its behavior is enhanced if a passive damping treatment is applied to the arm structure. This is important in light of the practical limitations on the bandwidth of actuators and the speed of computers to actively control the high frequency modes of the flexible arm. The regulator and damping treatment are both described further in the

Force must be applied by the end of the flexible arm to achieve bracing with friction. The current regulator is not so sensitive that the application of force with the end of the arm degrades the behavior. Force control is important to maintain the braced condition, however, and will be the subject of future research.

TRAJECTORY PLANNING FOR FLEXIBLE MANIPULATORS

Today, most trajectory planning algorithms do not consider the dynamics of manipulators, rather constant and/or piece wise constant accelerations for the overall task are used and an overall maximum allowable speed is set. [2,3,4]. However, robotic manipulators are highly nonlinear dynamic systems, so it is expected that affordable accelerations and decelerations and maximum speeds will vary as a function of states. For the traditional schemes to work, the trajectory must be planned for the worst possible case. The capabilities of the system will be used only a small part of the time. Bobrow et.al. [5] first reported that for every point on the path there is an associated maximum allowable speed and maximum affordable acceleration and deceleration, and these values can drastically vary from one state to another. Incorporating the manipulator dynamics into the trajectory planning, the minimum time trajectories were found for different manipulator models [5,6] with limited actuator capabilities moving along pre-defined paths. Shin and McKay [7] solved the same problem independently.

Light-weight manipulators with the same actuator capabilities will be faster. The main problem associated with the light-weight structures is the flexible vibrations. Fig. 1 conceptually shows the performance improvement in terms of increased speed.

In this section we show the performance improvements due to

1. Use of light-weight arms
2. Incorporating the manipulator dynamics into trajectory planning level.

Flexible Manipulator Dynamic Model In Joint And Path Variables

A general dynamic modelling technique for flexible robotic manipulators was developed by Book using a recursive Lagrangian-assumed modes method. Homogeneous transformation matrices are used for kinematic relations of the system [8]. A two link flexible robotic manipulator is modelled using that technique. In the model no actuator dynamics are considered, rather the net torque input to the links is considered as the input variable. No friction at joints nor in the structural vibrations is considered. Flexibility of each link is approximated with one assumed mode for each link. The dynamic model of the manipulator may be expressed in general terms as:

$$[J]_{4 \times 4} \ddot{q} = f(q, \dot{q}) + Q \quad (1)$$

where

$$\begin{aligned} \underline{q}^T &: [\theta_1, \theta_2, \delta_1, \delta_2] && \text{Angles and modes} \\ \underline{Q}^T &: [T_1, T_2, 0, 0] && \text{Net input torques} \\ [J] &_{4 \times 4} && \text{Generalized Inertia Matrix} \\ \underline{f}^T &: [f_1, f_2, f_3, f_4] && \text{Nonlinear dynamic terms} \end{aligned}$$

The problem is to find the minimum time trajectories for a given manipulator with limited actuator capabilities moving along a fixed path, with state constraints (bounded flexible vibration constraint). Once the path to be moved along is specified

$$S = S(x, y) \quad (2)$$

From inverse kinematic formulation, the corresponding joint angles can be found as

$$\underline{\theta} = \underline{\theta}(s), \quad \underline{\theta}^T = [\theta_1, \theta_2, \dots] \quad (3)$$

Similarly, once the speed along the path is known $S(s)$

$$\dot{\underline{\theta}} = \dot{\underline{\theta}}(s, \dot{s}) \quad (4)$$

and

$$\ddot{\underline{\theta}} = \ddot{\underline{\theta}}(s, \dot{s}, \ddot{s}) \quad (5)$$

Knowing the relations (3),(4),(5) in analytical or numerical form, the manipulator dynamics in part can be expressed in path variables.

$$\begin{bmatrix} C_{11}(s, \delta) \\ C_{12}(s, \delta) \\ \dots \\ C_{21}(s, \delta) \\ C_{22}(s, \delta) \end{bmatrix}_{2 \times 1} \ddot{S} = \begin{bmatrix} T_1 \\ T_2 \\ \dots \end{bmatrix} - \begin{bmatrix} C_{21}(s, \dot{s}, \delta, \dot{\delta}, \ddot{\delta}, \vec{e}_t, \vec{e}_n, \rho) \\ C_{22}(s, \dot{s}, \delta, \dot{\delta}, \ddot{\delta}, \vec{e}_t, \vec{e}_n, \rho) \end{bmatrix} \quad (6.a)$$

$$\begin{bmatrix} \delta_1 \\ \dots \\ \delta_2 \end{bmatrix} = \begin{bmatrix} J_{33} & J_{34} \\ \dots & \dots \\ J_{43} & J_{44} \end{bmatrix}^{-1} \begin{bmatrix} f_3 - g_3 + h_1(s, \dot{s}, \vec{e}_t) \\ \dots \\ f_4 - g_4 + h_2(s, \dot{s}, \vec{e}_t) \end{bmatrix} \quad (6.b)$$

$$f_i = f_i(s, \dot{s}, \delta, \dot{\delta}) \quad (7)$$

$$g_i = g_i(s, \dot{s}, \vec{e}_t, \vec{e}_n, \rho) \quad (8)$$

$$J_{ij} = J_{ij}(s, \delta) \quad (9)$$

\vec{e}_t, \vec{e}_n : Unit Tangential and normal Vectors along the path
 ρ : Curvature of the path at any point.

Notice that flexible modes also affect the position of the end effector, but are not included in the definition of the path. This is mainly due to the fact that we do not have a "direct" control on the flexible vibrations and would like to keep them as small as possible in general.

Formulation Of The Near Minimum Time Trajectory Problem

Using the classical variational calculus principles, the optimum control/programming problem may be formulated as following:

$$\text{Minimize } J = \int_0^{t_f} dt = \int_{S_0}^{S_f} \frac{ds}{\dot{s}}$$

$$\dot{S}(S_0) = \dot{S}_0$$

$$\dot{S}(S_f) = \dot{S}_f \quad \text{Initial and final states in}$$

path variables.

Subject to :

System dynamics, Equations (6a) and (6b),

Actuator constraints

$$T_{i \min}(\underline{\theta}, \dot{\underline{\theta}}) \leq T_i \leq T_{i \max}(\underline{\theta}, \dot{\underline{\theta}}) \quad i = 1, 2 \quad (2)$$

Dynamic inequality constraints on flexible modes

$$-a_i(t) \leq \delta_i(t) \leq b_i(t) \quad i=1, 2 \quad (3)$$

The constraints (3) naturally arise in flexible structures. If such a constraint is not imposed there is no guarantee on the accuracy of the end point along the path. At first the problem will be solved without considering these constraints. This solution will be used as a nominal solution for the trajectory modification step so that (3) are satisfied.

The solution method we use closely follows Bobrow et.al.'s method with some modifications for flexible manipulators. The solution of the above stated optimization problem follows: for any path $S(x,y)$ with given $\dot{S}_0(S_0), \dot{S}_f(S_f)$ to minimize J , \dot{S} should be as large as possible while satisfying the system dynamics and actuator constraints. In order to do so at any state on the path one should use maximum acceleration or deceleration. Then, the problem is reduced to finding the maximum accelerations and decelerations associated with each state of interest. It can be seen from equation (6a) that for each (S, \dot{S})

$$\ddot{S}_d \leq \ddot{S} \leq \ddot{S}_a \quad (4)$$

$$\ddot{S}_a = \min \left\{ \ddot{S}_{ai} \right\} \quad (5)$$

$$\ddot{S}_d = \max \left\{ \ddot{S}_{di} \right\} \quad (6)$$

Obviously, there may be some range of speeds associated with every point on the path that the system can no longer afford to satisfy all conditions (the S range that above inequality is violated.) Collection of these ranges defines the forbidden region on (S, \dot{S}) plane. The boundary between allowed and forbidden regions is constant for a given rigid manipulator for a given task: In the case of flexible manipulators, due to the coupling between equations (6.a) and (6.b) this boundary

is also a function of flexible modes, not only (S, \dot{S}) . So, depending on the time history of flexible modes and unpredictable disturbances the boundary will vary. This is not true in the rigid case where the true extremum can be found. At this point the problem is to find when to use maximum accelerations and maximum decelerations (i.e. to find the switching point(s)).

Finding switching points for flexible manipulators:

1. Integrate $\ddot{S} = \ddot{S}(x, y)$ from final state backward in time until it crosses the boundary into forbidden region or initial position, using maximum deceleration.
2. Integrate $\ddot{S}(x, y)$ Forward in time with maximum acceleration until the boundary is reached or the two curves crossed each other. If the two curves crossed each other before they enter forbidden region, then find that point. This is the last switching point and terminate the search. If not, then
3. Backup on the forward integrated curve and integrate forward with maximum deceleration until a the trajectory passes tangent to the boundary.
4. Then using the point as new starting point go to step two.

Notice that the last switching point is not the exact switching point because the flexible modes will not match at this point. That will cause one to miss the final state somewhat. Also, when searching for the switching points one has to move in a continuous manner in order to keep track of the flexible mode histories accurately. In that sense, the algorithm given at [5] has been modified for flexible robotic manipulators.

Simulation Results And Discussion

The two-link flexible manipulator model for task one (shown in Fig. 2a) was simulated for the two different cases in order to show the performance improvement achieved due to a light-weight system. In both cases actuators have same capabilities. It is found that weight reduction by a factor of 2 results in approximately a 60 % time improvement. This improvement, of course, slightly varies depending on the task. Joint actuator histories are shown in Fig. 4b and flexible mode responses are shown in Fig. 3b and 4c.

Task 2 (Shown in Fig. 2b) simulated for light-weight manipulator and results are shown Fig 5 a-c. The final trajectory is shown in heavy lines. One interesting point in this simulation is the fact that as soon as the manipulator end point enters the curvature the system must accelerate along the path in order to obey the constraints. In Fig. 5a the curve ab shows that right before the curvature the system is able to afford deceleration (aa' curve), but as end point enters the curvature, then the sudden appearance of a normal acceleration term in the dynamics of the system makes the difference.

ROLE OF PASSIVE DAMPING IN CONTROL OF FLEXIBLE MANIPULATORS

The central problem in achieving high-performance control of a flexible manipulator is the ability to "damp" the oscillations of the structure. This is made difficult by the presence in the structural elements of many (infinite) "modes" of vibration which are inherently lightly damped. Attempts to increase the characteristic speed of motion must deal with these lightly damped structural modes. The greater the characteristic speed desired the more modes that are significant. The modes become significant in two ways: 1. the oscillations themselves prolong the settling time or equivalently give greater dynamic errors and 2. attempts to actively control some modes result in instability of other modes, generally of high frequency.

Both of these phenomena are alleviated by increased structural damping which can be achieved by using "lossy" materials or by applying a surface treatment to the structural elements. Both have the effect of increasing the damping ratio associated with the various eigenvalues (or modes). It is interesting to note that for a manipulator with a payload that is heavy with respect to the weight of the manipulator only the first structural modal frequency is significantly changed by changes in payload weight. The higher frequency eigenvalues are essentially those of a beam that is pinned (for a point mass payload) at the payload end. Attempts to stiffen the manipulator by thickening the link walls do raise the frequency of the first structural mode but do relatively little to increase the frequency of higher modes. Thus if the higher modes are significant in the sense described in the preceding paragraph, beefing up the structure may do little good. Thus one is left with either actively controlling these higher frequency modes or increasing the structural damping.

The following discussion deals with: first the amount of damping available from constrained, single layer, passive-damping treatments; second, the theoretical effect of passive damping on the location of the closed loop eigenvalues; and third, some experimental results of an attempt to control a beam with and without a constrained layer passive damping treatment.

Characteristics of Constrained Layer Passive Damping

Constrained layer passive damping is achieved by sandwiching a thin layer of viscoelastic material between the surface of the structure and a stiff (but naturally elastic) constraining layer. When the structure deforms, shear induced plastic deformation is imposed in the viscoelastic layer which provides the desired mechanical damping effect. Lane [9] and others [10,11,12,13] have shown that the constraining layer is sectioned as shown in Figure 6 to achieve the greatest damping. The optimal section length does depend upon the frequency of oscillation that is being damped. Fortunately, the damping effect is rather broad band as shown in Fig. 7 and can be optimized to maximize the damping of those modes which are most troublesome in

the combined active/passive system; generally, the modes with frequencies just above the actively controlled mode(s). The amount of damping available can be increased by using a stiffer, hence heavier, constraining layer, but does not depend upon the thickness of the viscoelastic layer. Usually a very thin constraining layer would be used as dictated by fabrication requirements.

Effect of Passive Damping on the Location of Closed-Loop Eigenvalues

Lane[9] also studied the theoretical effect of passive damping on the location of closed-loop eigenvalues for a simple pinned-free beam that was actively controlled. In this control system, the torque at the driven end (pinned) was taken as a linear combination of four quantities, the angular velocity and position at the driven end and the linear velocity and position at the payload end. He considered the first 5 structural frequencies, i.e. twelfth order, in his beam model. Using root locus techniques the best he was able to do for the undamped case was for the dominant poles to be at $-5./+/-5.2j$ with a gain margin, for closed-loop poles at $-6.8+/-588j$, of 0.6 db. Using passive damping the comparable result was dominant poles at $-12.23+/-1.725j$ with gain margin for poles at $-61.17+/-585j$ of 8.9 db. Thus passive damping allowed faster, less oscillatory motion with gain margins that insured system stability.

The particular beam analyzed was 6 feet long, of aluminum, weighing 3.3 pounds, and with a payload of 100 pounds. The passive damping treatment, assumed to use a graphite fiber composite and a 3M brand viscoelastic material, added 0.3 pounds.

Experimental Results With Passive Damping

Alberts and Hastings [14] conducted an experiment with a flexible beam with modal control of the rigid body plus the first two structural modes. Angular position and rate at the driven end plus the output of two strain gages along the length were used with a Luenberger observer to attempt to reconstruct six states of this system. Gains were adjusted to maximize performance, guided in part by a linear quadratic optimization analysis. As higher performance was sought, unmodelled dynamics resulted in the behavior shown in Figure 8b for the untreated beam. When the same beam with the damping treatment was used the results of Figure 9(b) were obtained, illustrating the substantial effect of the damping in the case of model inaccuracy. These Figures are plots of strain for a step response in position. The beam is four feet long, with a 3/4 inch by 3/16 inch cross-section. The first two clamped-free frequencies with the payload in place are 2.0 and 13.5 Hz. The setup is described further below.

EXPERIMENTS IN REAL TIME CONTROL OF A FLEXIBLE MANIPULATOR

Current investigation of the control of flexible arms has progressed to the experimental phase. Initial results concerning the performance of an LQR optimal controller has been reported in other publications [15],[16]. Continuing investigations striving to achieve faster, tighter control differ significantly from the results anticipated by the analytical work. Diagnosis of the causes of the discrepancies has been carried out on simpler collocated control experiments, and will be discussed in this section. The following section describes the apparatus utilized in carrying out current experiments.

Experimental Apparatus

The setup is a complete laboratory for examining the control of flexible arms with frequencies as high as 100 Hz. The system consists of a flexible arm with payload, DC torque motor with servo-amp, A/D and D/A conversion for measurement sampling, signal conditioning, and 16 bit computer system for implementation of control algorithms. The physical configuration of the flexible arm, torque motor, and sensors is represented in Fig.10. The desired end point position can be input from an external analog signal generator, or from internal trajectory generation software.

The beam is a four foot long aluminum beam with a 3/4" by 3/16" cross section oriented for preferred bending in the horizontal plane. The beam was found to have natural frequencies of 7.3, 17.5, and 42 Hz in the first three modes when mounted in the experimental apparatus with payload. The control computer is an IBM series one system complete with floating point hardware, 64 megabyte hard storage, 24 channels of A/D conversion, and 2 channels of D/A conversion. The floating point hardware can accommodate either 32 or 64 bit manipulations. A typical value for 32 bit floating point multiplication is 17 microseconds.

The state-space model developed for the system considers the torque motor to be an ideal torque source introducing no attenuation or phase to the input. The torque motor is a brush type, permanent magnet, DC torque motor, driven by a large servo-amp. The servo-amp has an internal gain of 35,000 and is configured to maintain the motor current at a constant proportion of the commanded torque from the D/A on its input. Commutation of the armature has not introduced significant noise in tests to date.

Analysis Of Experimental Discrepancies

Experimental observations have indicated significantly lower damping ratios, and generally less stability than predicted by analytical models. Collocated control is being utilized as a tool for resolving the discrepancies, initial investigations have been aimed at identifying physical phenomena, which were not included in the model. Collocated controllers have

been investigated [17],[18],[19] more than the complex optimal controllers, and provide a better basis for identifying phenomena residing in the experimental apparatus.

Figure 8a is a time record of the strain measured at the base of the flexible arm with joint angle and angular velocity gains that result in slowly growing amplitudes of oscillations. Fig. 9a records the strain for the same gains; however, passive damping has been added to the arm. Past analysis of collocated feedback controllers utilizing joint angle and joint angular velocity have not predicted this result, and instead predict stable results for all gain combinations with velocity feedback. Fig. 11 depicts a closed loop root locus based on this type of analysis for increasing gains. The velocity gain is adjusted to be .2 of the angle feedback gain.

This reduction in stability from prediction has also been observed in optimal regulators applied to the same system [14]. Although many directions could be pursued in resolving the discrepancies, the investigation focused on three major facets of the physical hardware that were not contained in earlier models:

1. Servo-amp, motor combination as a torque source.
2. Sample and hold behavior of digital to analog converter.
3. Signal conditioning applied to tachometer to remove commutation noise.

These factors were investigated separately and cumulatively for their impact on the stability of the closed loop system via root locus analysis. A block diagram of the open loop transfer function from commanded torque to joint angular velocity is presented in Fig. 12a. Collocated feedback is depicted in the block diagram shown in Fig. 12b after reduction of the diagram in Fig. 12a to a transfer function $bT(s)$.

The transfer function from torque applied at the base of the flexible arm to the joint angular velocity can be described as a sum of clamped-free flexible modes over a sum of pinned-free flexible modes plus a rigid body mode with an appropriate scaling factor. The zeros which are measurement dependent, input relationships are adequately described by clamped-free modes, for a system employing collocated feedback. The transfer function includes one additional flexible mode in both the numerator and denominator of the transfer function than were plotted out. A four-pole filter was employed on the tachometer for reduction of commutation noise, and a suitable transfer function was developed for $Kv(s)$. A zero order hold was included on the input to the $T(s)$ transfer function to account for the digital conversion hardware.

The resultant closed loop transfer function could then be examined by varying the gains, and monitoring the resultant pole variations. The torque behavior of

servo-amp/motor combination was the least significant, or the most ideal of the factors considered and was included in the development of Fig. 11. Sampling and holding the commanded torque did have a destabilizing effect; however, over the range of sampling periods effected in the experiment it alone did not explain the observed trends. The filter utilized on the tachometer was the most destabilizing influence as it drastically alters the departure angle from the open loop poles. The frequency of the filter poles are approximately 30 times higher than the flexible frequencies of interest, yet surprisingly still strongly affect the stability. The proximity of the flexible poles to the imaginary axis makes this extremely important in accurately describing the behavior.

Optimal controllers implemented to date have increased the gain margin [16], but design approaches have not attempted to account for the impact of the hardware used in implementing the controllers.

Fig. 13 shows the results of including both the sample/hold and signal conditioning in the transfer function. Rigid body modes are omitted for clarity. The cross over frequency for the case without passive damping is roughly 122 rad/sec which agrees very well with the observed instability depicted in Fig. 8a. Modal damping ratios without the addition of passive damping have been measured to fall between .005 and measured damping ratios to approximately .06. The dashed line is in accordance with the difference in stability observed in Fig. 9a, and adds credence to the analytical results.

CONCLUSIONS

The various approaches described above are complimentary but may not in all cases to be used together. Analytical and experimental approaches are both essential to progress on the control of lightweight arms. More complete experiments on multi-link, multi-joint arms are under development. The greatest advantage to the suite of techniques seems to be for large arms where the motion sought naturally separates into gross and fine motions with high bandwidth. Hardware consistent with this situation is under design.

REFERENCES

1. Book, Wayne, "The Bracing Strategy for Robot Operation," Joint IFToMM-CISM Symposium on the Theory of Robots and Manipulators, Udine, Italy, June, 1984.
2. Kahn, M.E. and B. Roth, "The Near-Minimum Time Control of Open-Loop Articulated Kinematic Chains," Journal of Dynamic Systems, Measurement, and Control, ASME Trans., Vol. 93, No. 3, Sept 1971, pp 141-171.
3. Luh, J.Y.S. and C.S. Lin, "Optimum Path Planning For Mechanical Manipulators," Journal of Dyn. Syst. Measurement and Control, ASME Trans., Vol. 102, No. 2, June, 1981, pp 142-151.
4. Luh, J.Y.S. and M.W. Walker, "Minimum-time Along the Path for a Mechanical Manipulator," Proc. of IEEE Conf. on Decision and Control, Dec. 1977, New Orleans, LA, pp 755-759.

5. Bobrow, J.E., S. Dubowsky, and J.S.Gibson, "On the Optimal Control of Robotic Manipulators with Actuator Constraints," Proc.of 1983 ACC, San Francisco, CA June, 1983, pp 782-787.

6. Dubowsky, S., Z. Shiller, "Optimal Dynamic Trajectories For Robotic Manipulators," Fifth CISMIFToMM Symposium On The Theory And Practice Of Robotic Manipulators, June 26-29, 1984, Udine, Italy, pp96-103.

7. Shin, K.G. and M.D. McKay "Minimum-Time Control Of Robotic Manipulators With Geometric Path Constraints," IEEE Trans. on Automatic Control, Vol AC-30 No.6, June 1985, pp 531-541.

8. Book, W.J. "Recursive Lagrangian Dynamics of Flexible Manipulators," The International Journal of Robotics Research, MIT Press, v.3 n.3, pp. 87-101, Fall, 1984.

9. Lane, J.S., "Design and Control Principles for Flexible Arms Using Active and Passive Control," M.S. Thesis, Dept. of Mechanical Engr., Georgia Institute of Technology, 1984.

10. Plunket, R. and C.T. Lee, "Length Optimization for constrained Viscoelastic Layer Damping," J. Acoust. Soc. of Amer., Vol. 48, No. 1, 1970, pp 150-161

11. Kerwin, E.M. Jr., "Damping of Flexural Waves by a Constrained Viscoelastic Layer," J. Acoust. Soc. Amer., V. 31, N. 7, July, 1959, pp. 952-962.

12. Nashif, A.D. and T. Nicholas, "Vibration Control by Multiple-Layered Damping Treatment," Shock and Vib. Bull., N. 41, Part 2, Dec. 1970, pp 121-131.

13. Torvik, P., "The Analysis and Design of Constrained Layer Damping Treatments," Damping Applications for Vibration Control, P. Torvik, Ed., ASME, NY, 1980.

14. Alberts, Thomas, G. Hastings, W. Book, and S. Dickerson, "Experiments in Optimal Control of a Flexible Arm with Passive Damping," Fifth VPI&SU/AIAA Symposium on Dynamics & Control of Large Structures, Blacksburg, VA, June 12, 1985.

15. G. Hastings and W. Book, "Experiments in the Control of a Flexible Robot Arm," ROBOTS 9 Exposition & Conference, Detroit, MI, June 2, 1985.

16. G. Hastings and W. Book, "Experiments in the Optimal Control of a Flexible Manipulator," Proceedings of the 1985 American Control Conference, July, 1985.

17. W. Book, "Modelling, Design and Control of Flexible Manipulator Arms," Ph.D. Dissertation, Dept. of M.E., M.I.T., April, 1974.

18. G. Martin, "On the Control of Flexible Mechanical Systems," Ph.D. Thesis, Stanford U., 1978.

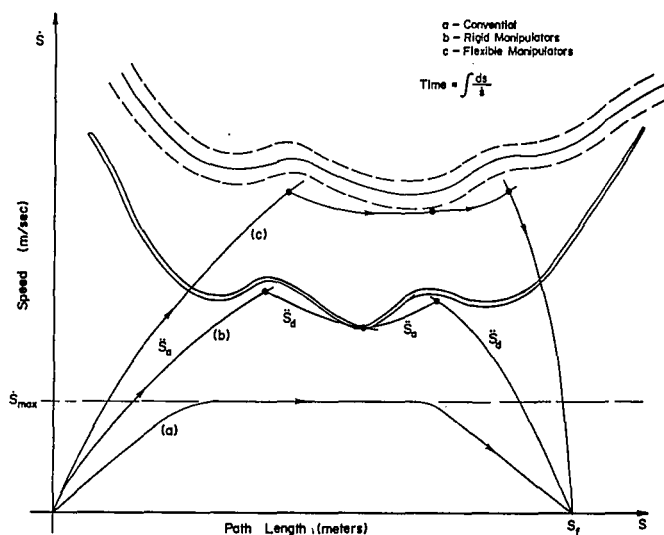


Fig. 1 Three different trajectory plans.

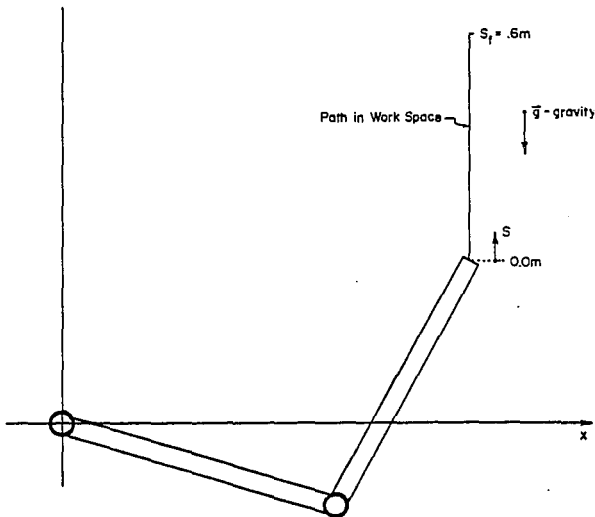


Fig. 2a Task 1 in (x,y) plane.

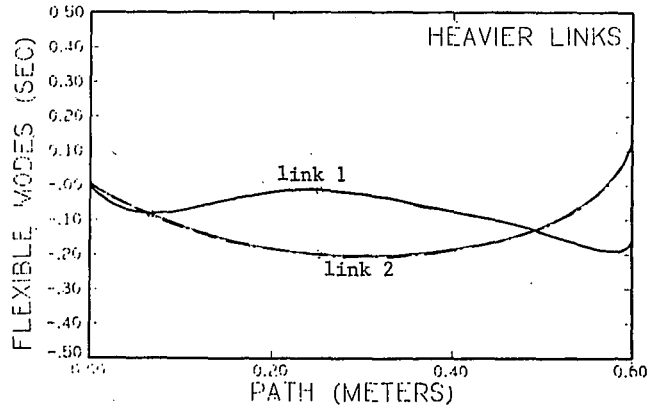


Fig. 3b Flexible modes for Task 1.

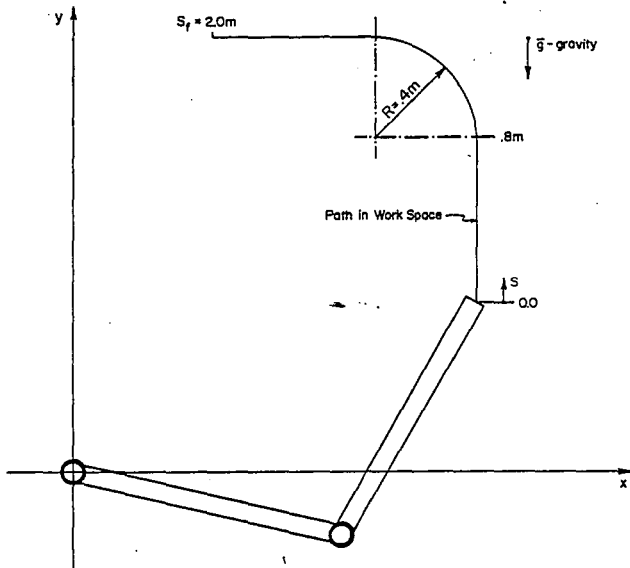


Fig. 2b Task 2 in (x,y) plane.

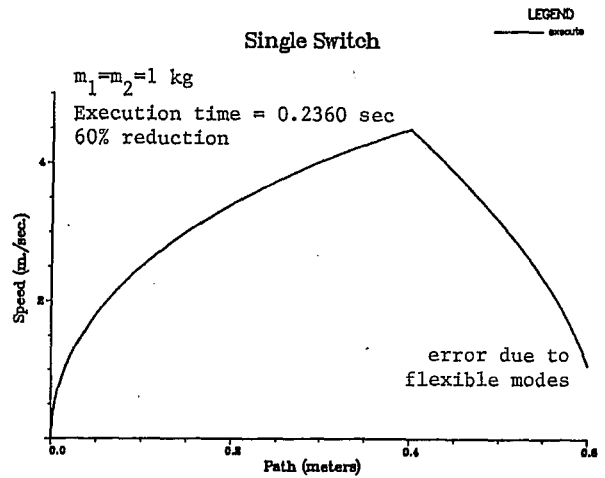


Fig. 4a Trajectory in (s,s) plane for Task 1 (light links)

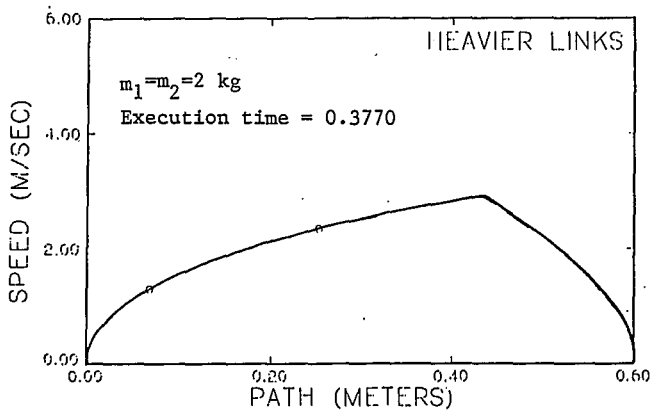


Fig. 3a Trajectory in (s,s) plane for Task 1 (heavy links).

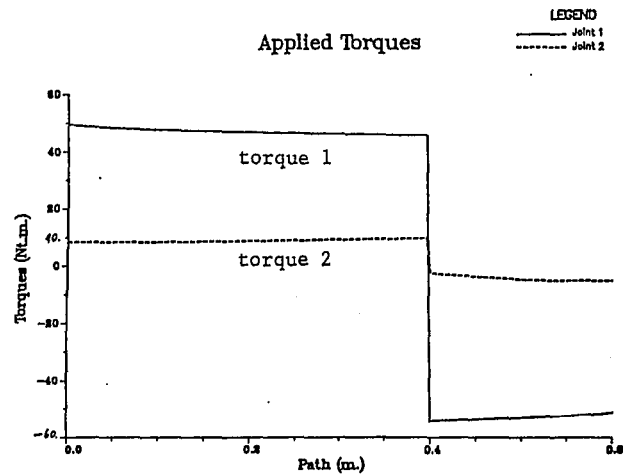


Fig. 4b Actuator torque histories for Task 1.

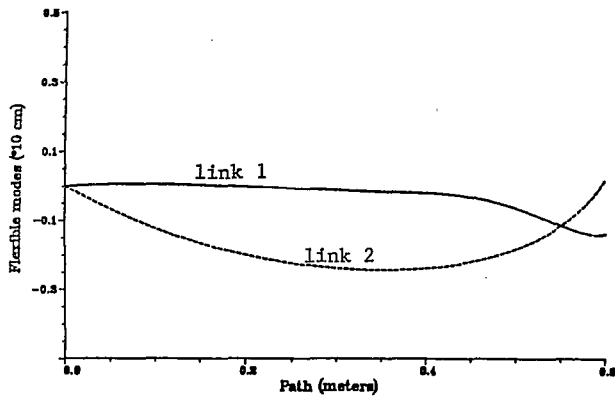


Fig. 4c Flexible modes for Task 1 (light links).

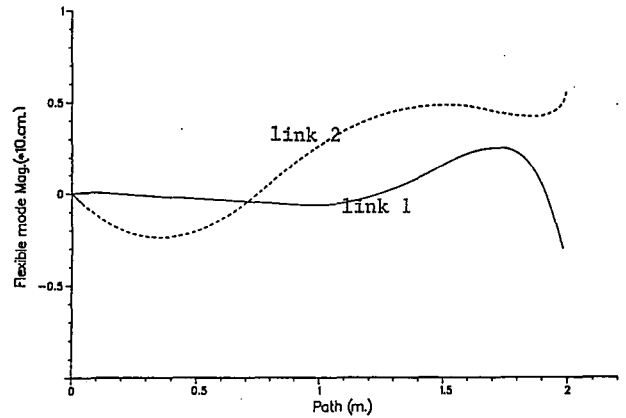


Fig. 5c Flexible modes for Task 2.

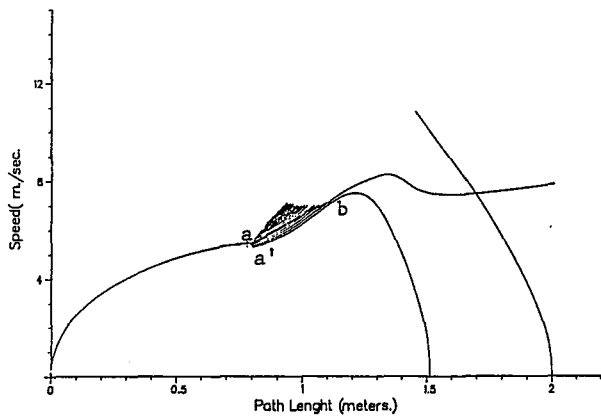


Fig. 5a Finding the switching points for Task 2.

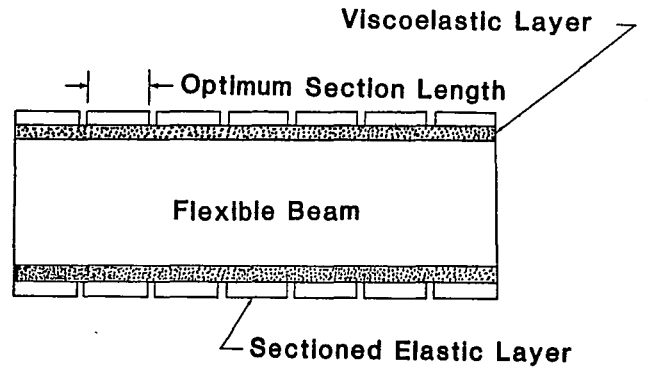


Fig. 6 Length optimized constraining layer.

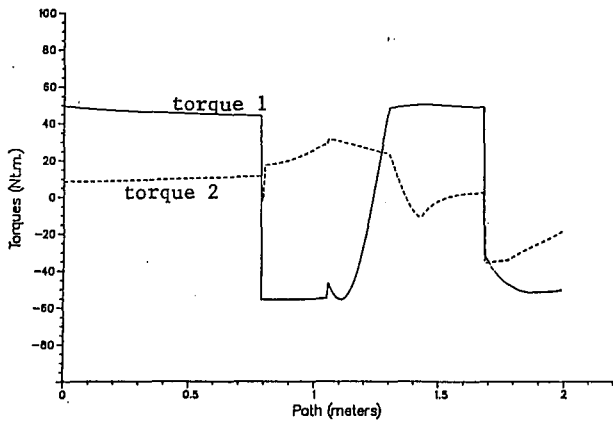


Fig. 5b Torque histories for Task 2.

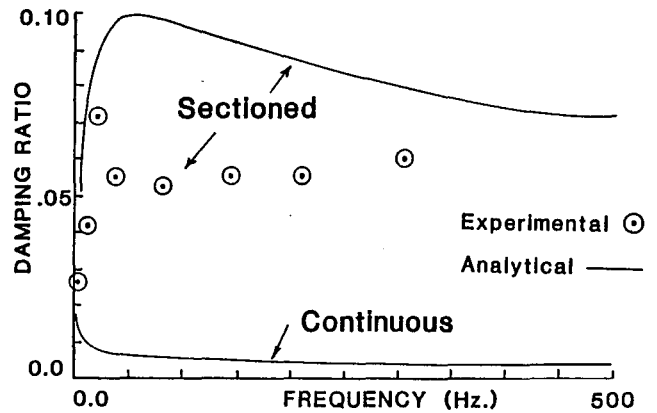


Fig. 7 Comparison of sectioned and continuous constraining layer treatments.

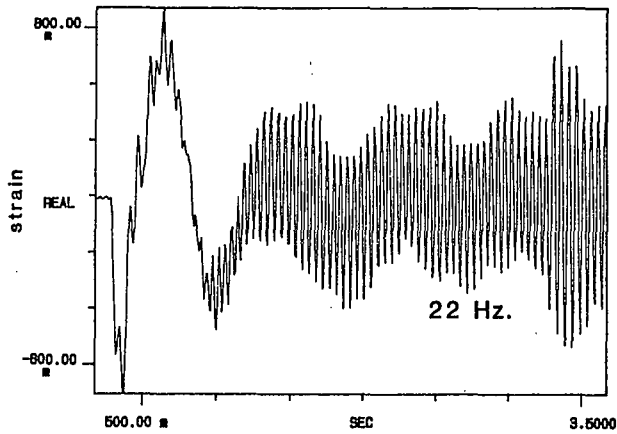


Fig. 8a Unstable system with colocated feedback only without passive damping.

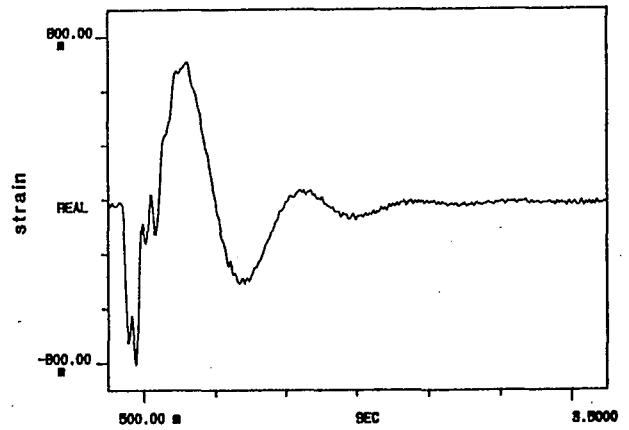


Fig. 9a System stabilized by addition of passive damping, colocated feedback only.

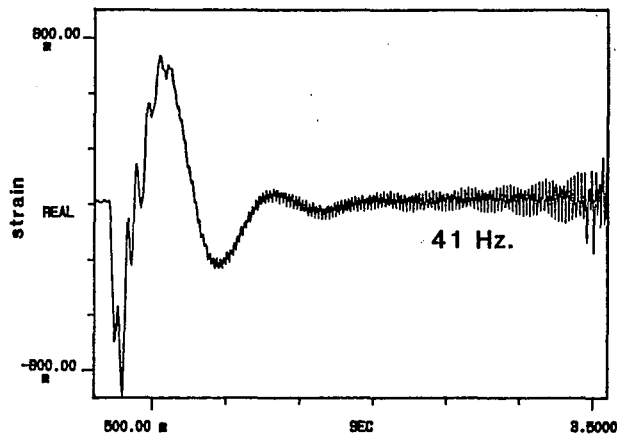


Fig. 8b Unstable system with modal feedback without passive damping.

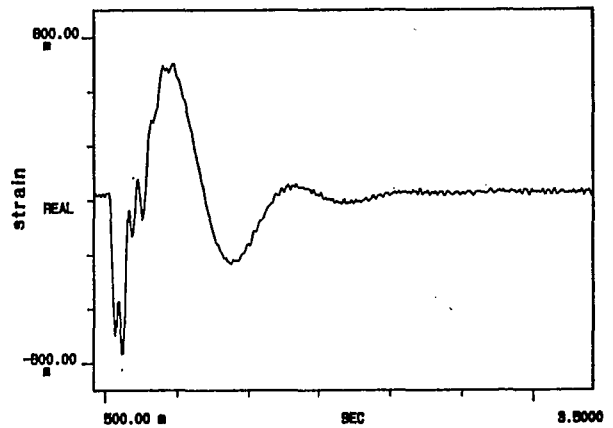


Fig. 9b System stabilized by addition of passive damping with modal feedback.

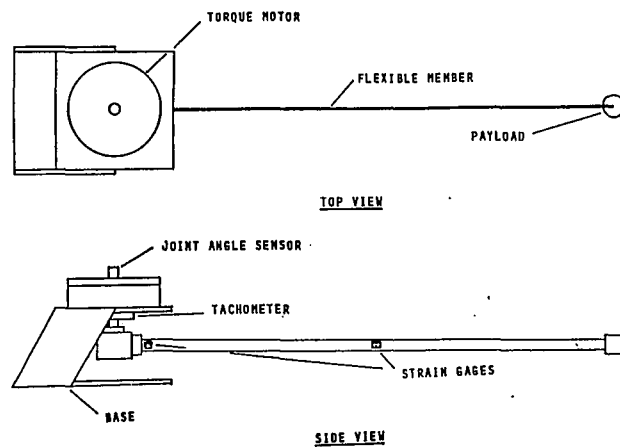


Fig. 10 Experimental one link arm.

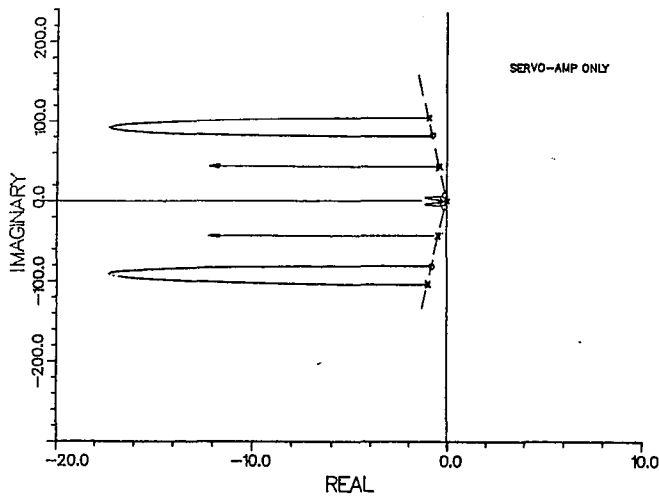


Fig. 11 Root locus for transfer function with servo-amp only.

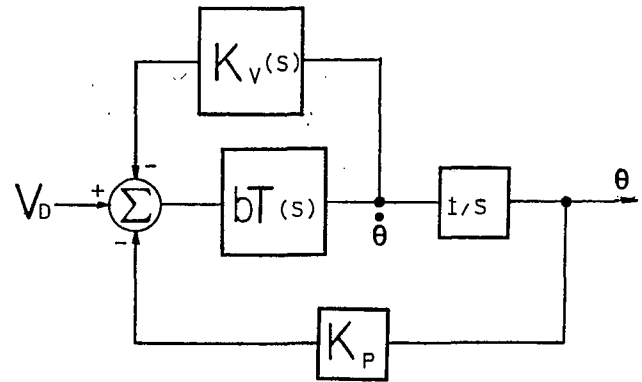


Fig. 12b Block diagram, collocated feedback.

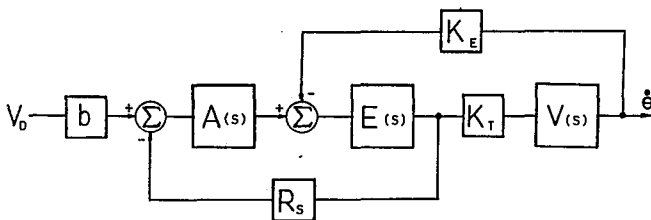


Fig. 12a Open loop block diagram. Symbols are:

- A(s) Amplifier transfer function, 35,000/s, v/v
- E(s) Motor electrical transfer function, 1/(Ls+R), amp/volt
- V(s) Torque to joint velocity transfer function, rad/sec-in-lb
- K_e Motor back emf constant, volt-sec/rad
- K_t Motor torque constant, in-lb/amp
- K_v(s) Velocity feedback transfer function, v-sec/rad
- K_p Joint angle feedback gain, volt/rad
- b Input gain, volt/volt
- V_d Desired torque voltage
- R_s Current sense resistor
- T(s) Open loop transfer function

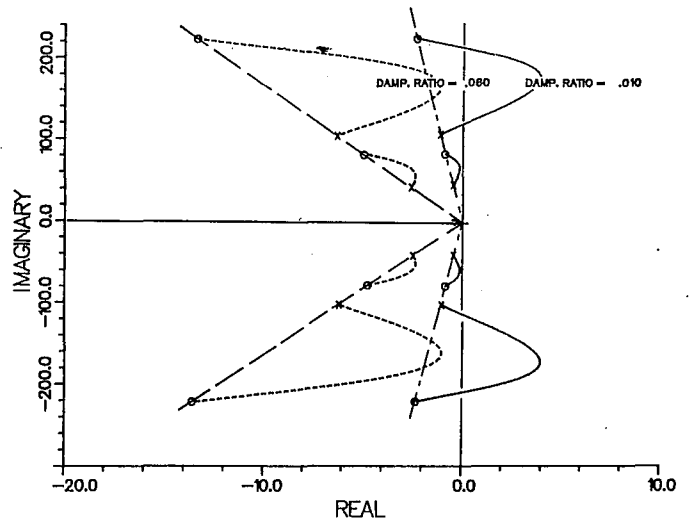


Fig. 13 Root locus for transfer function with filter, sampling, and servo-amp.